Robert Powers Publications — Published Research - Department of Chemistry

2008

Tricarboxylic Acid Cycle-Dependent Regulation of *Staphylococcus epidermidis* Polysaccharide Intercellular Adhesin Synthesis

Marat R. Sadykov
University of Nebraska—Lincoln

Michael E. Olson
University of Nebraska Medical Center

Steven M. Halouska
University of Nebraska-Lincoln, halouska@huskers.unl.edu

Yefei Zhu
University of Nebraska - Lincoln

Paul D. Fey
University of Nebraska Medical Center, pfey@unmc.edu

See next page for additional authors

Follow this and additional works at: http://digitalcommons.unl.edu/chemistrypowers

Authors

Marat R. Sadykov, Michael E. Olson, Steven M. Halouska, Yefei Zhu, Paul D. Fey, Robert Powers, and Greg A. Somerville

Tricarboxylic Acid Cycle-Dependent Regulation of *Staphylococcus epidermidis* Polysaccharide Intercellular Adhesin Synthesis[∇][†]

Marat R. Sadykov,[1] Michael E. Olson,[2] Steven Halouska,[3] Yefei Zhu,[1] Paul D. Fey,[2] Robert Powers,[3] and Greg A. Somerville[1]*

Department of Veterinary and Biomedical Sciences, University of Nebraska—Lincoln, Lincoln, Nebraska 68583-0905[1]; Department of Pathology and Microbiology, University of Nebraska Medical Center, Omaha, Nebraska 68198-6280[2]; and Department of Chemistry, University of Nebraska—Lincoln, Lincoln, Nebraska 68522-0304[3]

Staphylococcus epidermidis is a major nosocomial pathogen primarily infecting immunocompromised individuals or those with implanted biomaterials (e.g., catheters). Biomaterial-associated infections often involve the formation of a biofilm on the surface of the medical device. In *S. epidermidis*, polysaccharide intercellular adhesin (PIA) is an important mediator of biofilm formation and pathogenesis. Synthesis of PIA is regulated by at least three DNA binding proteins (IcaR, SarA, and σ^B) and several environmental and nutritional conditions. Previously, we observed the environmental conditions that increased PIA synthesis decreased tricarboxylic acid (TCA) cycle activity. In this study, *S. epidermidis* TCA cycle mutants were constructed, and the function of central metabolism in PIA biosynthesis was examined. TCA cycle inactivation altered the metabolic status of *S. epidermidis*, resulting in a massive derepression of PIA biosynthetic genes and a redirection of carbon from growth into PIA biosynthesis. These data demonstrate that the bacterial metabolic status is a critical regulatory determinant of PIA synthesis. In addition, these data lead us to propose that the TCA cycle acts as a signal transduction pathway to translate external environmental cues into intracellular metabolic signals that modulate the activity of transcriptional regulators.

Staphylococcus epidermidis is the most frequently isolated nosocomial pathogen from the blood cultures of adult and pediatric intensive care unit patients in the United States of America (48). Frequently, *S. epidermidis* infections involve the formation of a biofilm on the surfaces of biomaterials (e.g., catheters) (77). A biofilm is a complex aggregation of bacteria usually encapsulated by an adhesive exopolysaccharide matrix. The exopolysaccharide matrix provides structural stability to the biofilm, enhanced adhesion to surfaces, and protection from host defenses and antibiotics (2, 50, 79). In *S. epidermidis*, the exopolysaccharide facilitating bacterial adherence in a biofilm is polysaccharide intercellular adhesin (PIA). PIA is an *N*-acetylglucosamine polymer (44) of at least 130 residues (42) whose synthesis requires the enzymes encoded by genes in the intercellular adhesin (*ica*) operon (*icaADBC*) (27). The synthesis of PIA is required for the maturation of biofilms (27), important for evasion of the host innate immune system (79, 80), and critical in biomaterial-associated infections (55, 57).

Bacteria live in environments subject to rapid changes in the availability of the nutrients necessary to provide energy and biosynthetic intermediates for the synthesis of macromolecules. Consequently, bacterial survival depends on the ability to regulate expression of genes coding for enzymes required for growth in the altered environment. In pathogenic bacteria, adaptation to an altered environment often includes activating transcription of virulence genes; hence, synthesis of many virulence determinants is regulated by environmental/nutritional signals (e.g., nitrogen, iron, and calcium) (47). Because PIA is the most important virulence determinant of *S. epidermidis* (2, 7, 38, 56, 57, 84), it is not surprising that PIA synthesis is regulated by environmental and nutritional signals (13, 16, 18, 22, 53).

Regulation of the *icaADBC* operon is complex, involving at least two DNA binding proteins (IcaR and SarA) and the alternative sigma factor σ^B. IcaR binds immediately 5′ to the *icaA* transcriptional start site and represses transcription of the *ica* operon (9, 29). SarA is an essential positive effector of *icaADBC* transcription that binds to the *icaA* promoter region (26, 74). σ^B affects PIA synthesis indirectly by regulating the expression of *icaR* (34, 35, 52). In addition, the *luxS* quorum-sensing system has a minimal effect on PIA synthesis and biofilm formation; however, the mechanism remains to be determined (82).

In *Staphylococcus aureus*, σ^B is activated during stress conditions and growth phase transitions (3, 81). Because *S. epidermidis icaADBC* transcription and PIA synthesis are induced by environmental and nutritional stresses, stress-dependent activation of σ^B has been a focal point of research into the environmental regulation of PIA synthesis and biofilm formation (10, 26, 35). Importantly, σ^B does not respond directly to environmental signals; therefore, a second area of research interest has focused on identifying the regulatory network controlling σ^B activation, which is involved in responding to environmental signals. The activation of σ^B involves an anti-sigma factor (RsbW) and an anti-anti-sigma factor (RsbV) and resembles the process in the closely related organism *Bacillus subtilis* (35). In the absence of environmental stimuli, σ^B is bound in a complex with RsbW. Stress-inducing stimuli are hypothesized to activate the RsbU phosphatase to dephosphorylate (activate) the anti-anti-sigma

TABLE 1. Bacterial strains, bacteriophage, and plasmids used in this study

Bacterial strain, bacteriophage, or plasmid	Relevant properties[a]	Source or reference
Bacterial strains		
DH5α	*E. coli* cloning host	Invitrogen
RN4220	*S. aureus* restriction-deficient strain 8325-4	49
1457	*S. epidermidis* biofilm-forming strain	43
1457-*acnA*	Strain 1457 *acnA* inactivated mutant; Min[r]	This study
1457-*citZC*	Strain 1457 *citCZ* deletion mutant; Erm[r]	This study
1457-Δ*ica*	Strain 1457 *icaADBC* deletion mutant; Tmp[r]	26
1457-*icaR*	Strain 1457 *icaR* inactivated mutant; Min[r]	26
1457-*sigB*	Strain 1457 *sigB* inactivated mutant; Tmp[r]	26
1457-*sarA*	Strain 1457 *sarA* inactivated mutant; Min[r]	26
Bacteriophage 71	*S. epidermidis* transducing phage	15
Plasmids		
pCL15	Expression vector; derivative of pSI-1; Cam[r]	Chia Lee
pEC4	pBluescript II KS(+) with *ermB* inserted into ClaI site; Amp[r] Erm[r]	5
pJF12	Plasmid pCR2.1 containing *tetM*; Amp[r] Min[r]	J. Finan and G. Archer
pGEM-T	*E. coli* TA cloning vector; Amp[r]	Promega
pMRS2	pCL15 with *acnA* gene under the control of the P$_{spac}$ promoter; Cam[r]	This study
pMRS5	Derivative of pTS1-d with *citZC::ermB* fragment; Amp[r] Cam[r] Erm[r]	This study
pNF103	pUC19 with 1.7-kb internal fragment of *acnA*; Amp[r]	This study
pNF117	pNF103 with *tetM* inserted into EcoRI site; Amp[r] Min[r]	This study
pNF118	pRO6448::pNF117; Amp[r] Erm[r] Min[r]	This study
pRO6448	pE194(ts) with AluI fragment (*oriT*) of pC221 cloned into the unique ClaI site; Erm[r]	51
pTS1	Shuttle vector; pE194^{ts}; ColE1; Amp[r] Cam[r]	24
pTS1-d	Derivative of pTS1 with deletion of plasmid-encoded 3′ region of *ermC*	This study
pUC19	*E. coli* cloning vector; Amp[r]	83

[a] Amp[r], ampicillin resistant; Cam[r], chloramphenicol resistant; Erm[r], erythromycin resistant; Min[r], minocycline resistant; Tmp[r], trimethoprim resistant; ts, temperature-sensitive origin of replication.

factor RsbV, which then binds RsbW in a competitive manner to increase the concentration of free σ^B (34, 35). Based on several published studies, it seems likely that the σ^B posttranslational regulatory network is responsible for responding to some environmental stresses (i.e., osmotic stress) but is only minimally involved in responding to nutritional signals (e.g., glucose), suggesting that there are other means for *S. epidermidis* to "sense" nutritional signals (18, 35, 52).

Previously, we observed the environmental and nutritional signals that enhance PIA synthesis also repress tricarboxylic acid (TCA) cycle activity, leading us to hypothesize that repression of TCA cycle activity would increase PIA accumulation (78). To test this hypothesis, we incubated *S. epidermidis* strain 1457 with very low concentrations of fluorocitrate, which minimally inhibited TCA cycle activity, and determined the amount of cell-associated PIA. As the concentration of fluorocitrate in the culture medium was increased, the amount of PIA produced increased proportionally (78). Fluorocitrate is a highly toxic compound when metabolized to 4-hydroxy-*trans*-aconitate by the TCA cycle enzyme aconitase, severely limiting the usable concentration range (40, 46). In the present study, we overcame this limitation by genetically inactivating the aconitase gene in *S. epidermidis* strain 1457. The aconitase mutant and complemented strains permitted a detailed analysis of the function of central metabolism in PIA synthesis.

MATERIALS AND METHODS

Bacterial strains, bacteriophage, plasmids, and growth conditions. Bacterial strains, bacteriophage, and plasmids used in this study are listed in Table 1. *S. epidermidis* strain 1457 (43) was used in these studies because it is a known PIA-

and biofilm-producing strain. *Escherichia coli* strains were grown in 2× YT broth or on 2× YT agar (58). *S. aureus* and *S. epidermidis* strains were grown in tryptic soy broth without dextrose (TSB; BD Biosciences) supplemented with 0.25% glucose or on TSB containing 1.5% (wt/vol) agar. *S. epidermidis* cultures were inoculated 1:200 from overnight cultures (normalized for growth) into TSB, incubated at 37°C, and aerated at 225 rpm with a flask-to-medium ratio of 7:1. Bacterial growth was assessed by measuring the optical density at 600 nm or by determining the number of CFU ml^{-1}. Antibiotics were purchased from Fisher Scientific or Sigma Chemical and were used at the following concentrations: ampicillin (100 μg/ml for *E. coli*), chloramphenicol (8 μg/ml), erythromycin (8 μg/ml), minocycline (2 μg/ml), and trimethoprim (10 μg/ml).

***Staphylococcus epidermidis* mutant construction. (i) Aconitase (*acnA*) mutant.** A 1.7-kb internal PCR product of the *acnA* gene of *S. epidermidis* strain 1457 was amplified using primers 663 forward (contains a KasI restriction site) and 664 reverse (contains a PstI restriction site) (Table 2) and cloned into pGEM-T (Promega). The 1.7-kb PCR product was excised from pGEM-T by digestion with KasI and PstI and ligated into the KasI and PstI sites of pUC19 (83) to generate the plasmid pNF103. The *tetM* cassette from plasmid pJF12 (from J. Finan and G. Archer) was inserted into a unique EcoRI site of pNF103 at nucleotide position 856 of the 2,702-bp *acnA* gene to generate the pNF117 plasmid. The temperature-sensitive plasmid pROJ6448 (51) was digested with PstI and ligated into the unique PstI site of pNF117. The resulting temperature-sensitive plasmid pNF118 was passaged through *S. aureus* strain RN4220 and introduced into *S. epidermidis* strain 1457 by electroporation (59). Strain 1457 containing plasmid pNF118 was used to construct an *acnA*::*tetM* mutant as described previously (19). The resulting mutant was backcrossed into wild-type strain 1457 using transducing phage 71 (15). Inactivation of the *acnA* gene by *tetM* cassette was verified by PCR, Southern blot analysis (68), and enzymatic assays (64).

(ii) Citrate synthase (*citZ*) and isocitrate dehydrogenase (*citC*) double mutant. The genes coding for citrate synthase and isocitrate dehydrogenase are present in a two-gene operon and cotranscribed. To inactivate the *citZC* operon, a gene splicing by overlap extension technique was used to replace a 2-kb internal DNA region of *citZC* by the *ermB* gene. The *ermB* gene was amplified from pEC4 (5) using primers citC-r-ermB2 and citZ-f-ermB (Table 2), containing sequences homologous to the *citC* and *citZ* genes. Genomic DNA from *S. epidermidis* strain

TABLE 2. Oligonucleotide primers used in this study

Primer	Nucleotide sequence (5′→3′)
663 forward	GCGCGCGGCGCCGGGATATAAAATGGCTTCTA
664 reverse	GCGCGCCTGCAGACCAGCAAGCGCATAAGCTA
SERP1762(glmM)-f	CACCTGAATTGGCTTTTAAACTAGG
SERP1762(glmM)-r	TCAACACGATATTTGTCAGTCACTC
SERP1760(glmS)-f	GTGTGGAATTGTTGGTTATATTGGG
SERP1760(glmS)-r	GCTTCACGTGATAATGTTGAACC
glmU-f	CGATTATTCTGGCAGCAGGTAAG
glmU-r	CGATTGATACGTTGTTGCAAAGC
icaProbeforward	GACAGTCGCTACGAAAAG
icaProbereverse	CCGAATAATTTGTAAATTTCC
icaR-r	GGAGGCTCTAAAATACCAAGTCTC
icaR-f	GGTACGATGGTACTACACTTGATG
pgi-f	GCATGAACTAGATCAGCAAAAGGATATTG
pgi-r	GCTGTAAGAACAGAATAACGACCTCC
sarA-f	GGCTATTTCAAAAATCAATGACTGCTTTG
sarA-r	GCTTCTGTGATACGGTTGTTTACTC
sigB-f	CGAAAGAGTCGAAATCAGCTAGTG
sigB-r	GTGAAACATGCATTTGACTAAGACC
SalI-SD-acnA-f	CTAAGTCGACAATATCAAGGGGGATATAAAATGGCTTC
SacI-acnA-r	CAAGAGCTCATGACTG CTTGTACTCAATAGTGAG
pCL15-f	GTTCTACATCCAGAACAACCTCTGC
pCL15-r	GAAATGATGACCTCGTTTCCACCG
citC-r-ermB2	GACGTTCTGTACCTTCTTTAGGCGACTCATAGAATTATTTCCTCCC
citZ-f-ermB	CACTTTGAGGAGTATGTGACGAAGGAGGGATTCGTCATGTTG
phoP-BamHI	GGaGGATCCACGTACAGTCTTTATCAATTTAGGTTGC
ermB-citC-f2	GGAAATAATTCTATGAGTCGCCTAAAGAAGGTACAGAACGTCTAGTAAGAG
ansP-SacI	GCAGAGCTCACTAAGTGTCGATGTAAATTTTATCGTGC
ermB-citZ-r	GACGAATCCCTCCTTCGTCACATACTCCTCAAAGTGCTTGTATAC

1457 was used as a template for PCR amplification of the DNA flanking the internal *citZC* region. Primers ansP-SacI and ermB-citZ-r (Table 2) were used for amplification of a 1.9-kb region of the *citZ* upstream region. A 1.7-kb region of the *citC* downstream region was amplified using phoP-BamHI and ermB-citC-f2 (Table 2). The resulting 4.6-kb PCR product consisted of a 1-kb *ermB* gene with DNA flanking the internal *citZC* regions. The 4.6-kb PCR product contained SacI and BamHI sites that were used for ligation into pTS1-d digested with SacI and BamHI to generate pMRS5. The temperature-sensitive plasmid pTS1-d is a derivative of pTS1 (24) with deletion of the plasmid-encoded 3′ region of the *ermC* gene. It was constructed by PCR amplification of pTS-1 DNA using primers pTS1dErm-f and pTS1dErm-r, and the resulting PCR product was self-ligated as described previously (45). Plasmid pMRS5 was used to construct a strain 1457 *citZC* double mutant (1457-*citZC::ermB*) (19). Allelic replacement of the internal region of *citZC* genes by the *ermB* cassette was verified by PCR and Southern blot analysis.

Construction of the complementation plasmid. Plasmid pCL15 (a kind gift of Chia Lee), containing a P_{spac} promoter, was used for the construction of an *acnA* complementation plasmid. The pMRS2 complementation plasmid was constructed by amplifying the 2.7-kb promoterless *acnA* gene from *S. epidermidis* strain 1457 using SalI-SD-acnA-f and SacI-acnA-r primers, followed by ligation of the PCR product into plasmid pCL15 digested with SalI and SacI. Plasmid pMRS2 was isolated from *S. aureus* strain RN4220 and electroporated into *S. epidermidis* strain 1457 (59). Plasmid pMRS2 was introduced into strain SE1457-*acnA* using transducing phage 71 (49). Induction of expression from the P_{spac} promoter was performed by supplementing bacterial cultures with isopropyl-β-D-thiogalactopyranoside (IPTG) (1 mM).

Measurement of acetic acid and glucose concentrations in culture medium. Aliquots of bacteria (2 ml) were centrifuged for 3 min at 14,000 rpm at 4°C, and the supernatants were removed and stored at −20°C until use. Acetate and glucose concentrations were determined with kits purchased from R-Biopharm and used according to the manufacturer's protocol.

Determination of NAD⁺, NADH, and ATP concentrations. Intracellular NAD^+ and NADH concentrations were determined with an enzymatic cycling assay kit (Biovision). Briefly, aliquots (5 to 20 ml) were harvested at 2, 3, 4, 5, and 6 h by centrifugation at 4°C for 10 min at 4,000 rpm. Bacterial pellets were suspended in 1 ml of extraction buffer (Biovision) and lysed using lysing matrix B tubes (Qbiogene) in a FastPrep instrument (Qbiogene). The lysate was centrifuged at 4°C for 5 min at 14,000 rpm. NAD^+ and NADH concentrations were determined according to the manufacturer's protocol and normalized to the cell density. All assays were performed in duplicate for two independent experiments.

Intracellular ATP concentrations were determined using the Enliten ATP assay (Promega). Briefly, 2×10^7 bacteria were collected at 2, 3, 4, 5, and 6 h, washed three times with 1 ml of phosphate-buffered saline, and suspended in 100 µl of phosphate-buffered saline. Bacteria were lysed by the addition of 900 µl of dimethyl sulfoxide (23). ATP concentrations were determined according to the manufacturer's protocol and normalized to the cell density. All assays were performed in duplicate for two independent experiments.

Determination of aconitase activity. Cell-free lysates of *S. epidermidis* were prepared as follows: aliquots of bacteria (2 ml) were harvested by centrifugation and suspended in 750 µl of lysis buffer containing 90 mM Tris (pH 8.0) and 100 µM fluorocitrate. The samples were lysed using lysing matrix B tubes (Qbiogene) in a FastPrep instrument (Qbiogene). The lysate was centrifuged for 5 min at 14,000 rpm and 4°C. Aconitase activity was assayed in the resulting cell-free lysate as previously described (63). One unit of aconitase activity is defined as the amount of enzyme necessary to give a ΔA_{240} min^{-1} of 0.0033 (1). Protein concentrations were determined by the method of Lowry (41).

PIA immunoblot assay. PIA accumulation was determined as described previously (78). Briefly, TSB medium containing 0.25% glucose was inoculated with equal numbers of bacteria from overnight cultures. The cultures were grown at 37°C, with a flask-to-medium ratio of 7:1, and aerated at 225 rpm. Every 2 h, equal numbers of bacteria (0.25 A_{600} unit) were harvested by centrifugation, and the PIA was extracted in 0.5 M EDTA (pH 8.0) by boiling for 5 min. Aliquots of PIA were applied to a polyvinylidene difluoride membrane (Immobilon-P; Millipore) and blocked with 5% skim milk overnight. The polyvinylidene difluoride membrane was incubated for 2 h with PIA-specific antiserum (generously provided by Michael Otto), which was followed by a 2-h incubation with an anti-rabbit immunoglobulin G peroxidase conjugate. The presence of PIA was detected using SuperSignal West Pico chemiluminescent substrate (Pierce). The integrated density values of bands on autoradiographs were determined with the TotalLab software (Nonlinear Dynamics Ltd.)

Northern blot analysis. Northern blot analysis of transcripts was performed as described previously (58), except that total RNA was isolated using the FastRNA Pro Blue kit (Qbiogene) and purified using an RNeasy kit (Qiagen). Oligonucleotide primers (Table 2) used in making DNA probes were designed using the *S. epidermidis* RP62A genome sequence (GenBank accession number CP000029). Probes for Northern blotting were generated by PCR amplification of unique internal regions of *glmM*, *glmS*, *glmU*, *icaD*, *icaR*, *pgi*, *sarA*, and *sigB* genes and labeled using the North2South random prime labeling kit (Pierce). Electrophoresis, transfer of the RNA to the Nytran SPC nylon membrane (Whatman), and hybridization were done using the NorthernMax kit (Ambion). Detection was performed using the chemiluminescent nucleic acid detection module (Pierce). When necessary, reprobing of blots was done according to the manufacturer's protocol.

NMR data collection, processing, and analysis. Nuclear magnetic resonance (NMR) samples were prepared from three independent cultures (50 ml) of *S. epidermidis* strains 1457 and 1457-*acnA* during the exponential growth phase (2 h) and postexponential growth phase (6 h) using [$^{13}C_6$]glucose (Cambridge

TABLE 3. Summary of metabolic differences identified in
S. epidermidis strains by NMR after 2 h of growth

Increased intracellular concn in the wild-type strain 1457[a]	Increased intracellular concn in strain 1457-*acnA*[a]	Similar intracellular concns in wild-type and 1457-*acnA* strains
Lactic acid	Valine	Acetate
Succinate	Leucine	Glucose
Glutamate	Lysine	Glucosamine
Glutamine	Citrate	Ethanol
Asparagine	Serine	Glucose-6-phosphate
Aspartate	Arginine	Inosine
	Fructose-6-phosphate	Adenosine
	Glucono-1,5-lactone	Xanthosine
	Acetaldehyde	*N*-Acetylglutamate
	Isoleucine	NAD
	Ornithine	Uridine
	UDP-*N*-acetylglucosamine	Alanine

[a] The intracellular concentration was considered to be increased when the percent difference in the NMR peak intensities was fivefold greater than the percent error observed in the peak intensities between the triplicate NMR spectra.

TABLE 4. Summary of metabolic differences identified in
S. epidermidis strains by NMR after 6 h of growth

Increased intracellular concn in the wild-type strain 1457[a]	Increased intracellular concn in strain 1457-*acnA*[a]	Similar intracellular concns in wild-type and 1457-*acnA* strains
Glutamine	Ethanol	Glucosamine-6-phosphate
Glutamate	Alanine	Glucose
Ornithine	Lactate	Ribose
Succinate	Acetate	Glucose-6-phosphate
Asparagine	Acetaldehyde	NAD
Aspartate	Citrate	UDP-glucuronate
γ-Aminobutanoate	UDP-*N*-acetylglucosamine	Ribose-5-phosphate
Isocitrate	Uridine	Inosine
Fructose-6-phosphate		Adenosine
		Xanthosine

[a] The intracellular concentration was considered to be increased when the percent difference in the NMR peak intensities was fivefold greater than the percent error observed in the peak intensities between the triplicate NMR spectra.

Isotope Laboratories) in place of glucose in the growth medium. Bacteria were rapidly harvested, lysed using lysing matrix B tubes (Qbiogene) in a FastPrep instrument (Qbiogene), and centrifuged to remove the cell debris. Samples were lyophilized, suspended in a 99.8% D_2O (Isotec) 50 mM phosphate buffer, and an aliquot (500 μl) was transferred to an NMR tube for analysis.

The NMR spectra were collected on a Bruker 500-MHz Avance spectrometer equipped with a triple-resonance, *z*-axis gradient cryoprobe. A BACS-120 sample changer with Bruker Icon software was used to automate the NMR data collection. Two-dimensional (2D) ^1H-^{13}C-heteronuclear single quantum coherence (^1H-^{13}C-HSQC) spectra were collected with a Bruker pulse sequence (HSQCE TGP), solvent presaturation, and relaxation delay of 0.5 s. A total of 1,024 data points with a sweep width of 4734.85 Hz and 64 data points with a sweep width of 13834.26 Hz were collected in the ^1H and ^{13}C dimensions, respectively. A total of eight dummy scans and 128 scans were used to obtain each of the 2D ^1H-^{13}C HSQC NMR spectra. Spectra were processed using the NMRPipe software package (17) and zero-filled with 2,048 and 1,024 points in the ^1H and ^{13}C dimensions, respectively. Additionally, the spectra were Fourier transformed, manually phased, and baseline corrected.

Spectra were analyzed using Primitive Interactive Peak Picker (PIPP) (20) to determine chemical shifts and peak intensities. The chemical shifts were divided into three groups (Tables 3 and 4) based on the intensities of similar peaks between the wild-type and *acnA* mutant strains during the exponential and postexponential phases of growth. Peak intensities were normalized for each spectrum by dividing by the average peak intensity. The triplicate data sets were then used to calculate average peak intensities for each peak observed in the 2D ^1H-^{13}C HSQC spectra for the wild-type and *acnA* mutant. Similarly, a percent error was calculated for each peak by dividing the standard deviation by the average peak intensity. The average peak intensities were then used to calculate a percent difference between the wild-type and *acnA* mutant. Peaks with calculated percent differences greater than five times the average percent error were considered to have increased concentrations in the wild-type or *acnA* mutant strains. Peaks with less than a fivefold deviation were considered similar. The peaks assigned to the same metabolite were required to have the same relative change in intensity in order to be classified as a metabolite with an increase in concentration.

NMR peaks were assigned to specific metabolites using the Madison Metabolomics Consortium Database (14) using a tolerance of 0.05 ppm and 0.50 ppm for ^1H and ^{13}C dimensions, respectively. The presence of metabolites and metabolic pathways were verified with the KEGG (31) and Metacyc (32) databases. NMR reference data available from the Madison Metabolomics Consortium Database is incomplete, so it is currently not feasible to assign every NMR resonance observed in the 2D ^1H-^{13}C HSQC NMR spectra to a *S. epidermidis* metabolite. It is also important to note that the combination of 2D ^1H-^{13}C HSQC NMR spectra with isotopically enriched (e.g., $[^{13}C_6]$glucose) cellular extracts enables the measurement of accurate metabolite concentration changes relative to one-dimensional ^1H NMR metabolomic methods alone. Generally, only compounds that are metabolic products of $[^{13}C_6]$glucose were detected.

Statistical analysis. The statistical significance of changes between wild-type and mutant strains (e.g., ATP concentrations) was assessed with the Student's *t* test. To determine whether a correlation existed between two physiological parameters, a correlation coefficient (ρ) was calculated.

RESULTS

Construction and characterization of an *S. epidermidis* strain 1457 aconitase mutant. Partial biochemical inhibition of TCA cycle activity in *S. epidermidis* increased the accumulation of PIA (78). Because fluorocitrate is very toxic, we were unable to completely block TCA cycle activity without killing the bacteria. To overcome this obstacle, we inactivated the TCA cycle in *S. epidermidis* strain 1457 by insertion of a *tetM* cassette into the gene encoding aconitase (*acnA*; also known as *citB*) and then assessed the effect on PIA synthesis. In *S. epidermidis*, aconitase is present as a sole copy on the chromosome; hence, inactivation of aconitase results in a nonfunctional TCA cycle. Inactivation of the aconitase gene in *S. epidermidis* strain 1457 by allelic replacement was genotypically verified by PCR and Southern blot analysis (data not shown) and phenotypically by aconitase enzymatic activity assays (Fig. 1A). In addition, overall TCA cycle function was assessed by measuring the accumulation and depletion of acetic acid from the culture medium of the wild-type, mutant, and complemented strains (Fig. 1D). (Acetic acid catabolism in staphylococci requires a fully functional TCA cycle [64, 65].) As expected, aconitase inactivation inhibited the postexponential oxidative catabolism of acetic acid (Fig. 1D). Of importance, when the concentration of acetic acid in the culture medium was plotted as a function of growth, the exponential growth phase rates of acetic acid accumulation in strains 1457 and 1457-*acnA* were equivalent (data not shown), suggesting that carbon utilization in both strains was proceeding through glycolysis and the acetate kinase/phosphotransacetylase pathway at a similar rate. The equivalent rate of acetic acid accumulation in strains 1457 and 1457-*acnA* was also supported by NMR metabolomic analysis (Table 3). If carbon flow through glycolysis were equivalent,
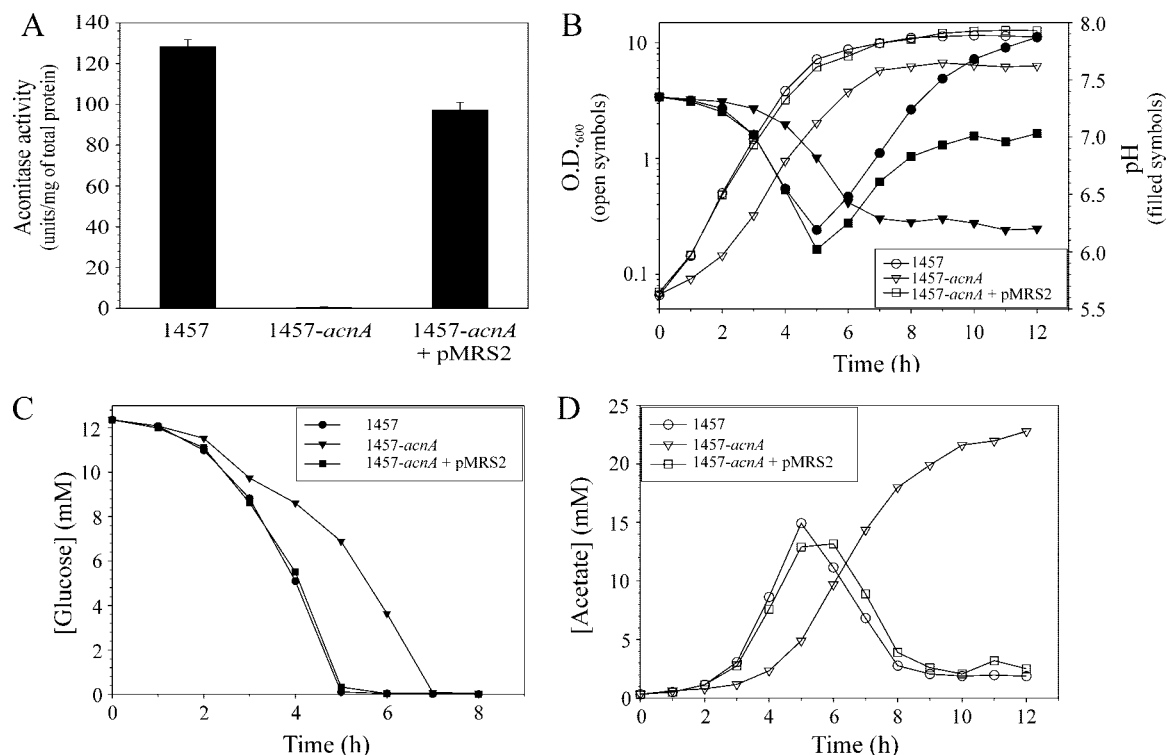
FIG. 1. Growth characteristics of the *S. epidermidis* strain 1457 aconitase mutant. (A) Aconitase activity of *S. epidermidis* strains 1457, 1457-*acnA*, and 1457-*acnA* containing pMRS2 (1457-*acnA* + pMRS2) was determined 6 h postinoculation. (B) Growth curves of wild-type strain 1457, aconitase mutant strain 1457-*acnA*, and strain 1457-*acnA* containing the complementing plasmid pMRS2 grown in TSB containing 0.25% glucose. At the indicated times, aliquots were removed, and the optical density at 600 nm (O.D.$_{600}$) was measured, and the pH of the culture medium was determined. (C) Temporal depletion of glucose from the culture medium of strains 1457, 1457-*acnA*, and 1457-*acnA* containing pMRS2. (D) Temporal accumulation and depletion of acetic acid in the culture medium of strains 1457, 1457-*acnA*, and 1457-*acnA* containing pMRS2. The results are representative of at least two independent experiments.

then it is reasonable to predict that the growth rate of the wild-type and aconitase mutant strains would also be equivalent. Surprisingly, the growth rate of strain 1457-*acnA* was lower than the growth rate of the isogenic wild-type strain, and this was reflected in the temporal depletion of glucose (Fig. 1C). This result was surprising because TCA cycle activity is repressed during the exponential growth phase when nutrients are abundant; thus, inactivating a repressed metabolic pathway should have minimal consequences. Restoration of the growth rate and the ability to catabolize acetate was accomplished by complementation of the strain 1457-*acnA* mutation with a plasmid (pMRS2) containing the *acnA* gene under the control of a P$_{spac}$ promoter (Fig. 1A to D). As a whole, these date demonstrate that *acnA* was inactivated, and this resulted in a metabolic block in the TCA cycle.

TCA cycle inactivation redirects carbon from growth into UDP-*N*-acetylglucosamine biosynthesis. When grown in the presence of a rapidly catabolizable carbon source, gram-positive bacteria repress the TCA cycle; hence, there is an accumulation of acidic secondary metabolites (e.g., acetate) in the culture medium. Derepression of the TCA cycle occurs upon depletion of the readily catabolizable carbon source(s) and coincides with the depletion of acetate from the culture medium. The processing of glucose through glycolysis and the resulting accumulation of acetate during substrate-level phosphorylation were equivalent in *S. epidermidis* strains 1457 and

1457-*acnA*; hence, the lower growth rate of strain 1457-*acnA* relative to the wild-type strain was likely due to a redirection of carbon and energy from growth into other cellular processes or metabolic pathways. If carbon and/or energy were diverted from growth to another metabolic pathway or process, then the number of bacteria produced per unit of glucose consumed should be lower in the aconitase mutant strain than in the wild-type strain. Plotting the glucose concentrations in the culture medium as a function of optical density at 600 nm for three independent experiments (Fig. 2) confirmed that fewer bacteria are produced per unit of glucose consumed by strain 1457-*acnA* than by strain 1457. These data strongly suggest that carbon and/or energy were diverted from growth into other cellular processes. To determine the metabolic pathways into which carbon might be redirected, we utilized NMR metabolomics to assess the metabolic status of strains 1457 and 1457-*acnA* in the exponential growth phase (2 h) and the postexponential growth phase (6 h) (see Fig. S1 and S2 in the supplemental material) (Tables 3 and 4). As expected, TCA cycle inactivation decreased the intracellular concentration of amino acids derived from TCA cycle intermediates (Asn, Asp, Gln, and Glu) and increased accumulation of the PIA biosynthetic precursor UDP-*N*-acetylglucosamine. Interestingly, TCA cycle inactivation resulted in an exponential-growth-phase accumulation of branched-chain amino acids relative to the wild-type strain (see Fig. S1 in the supplemental material)
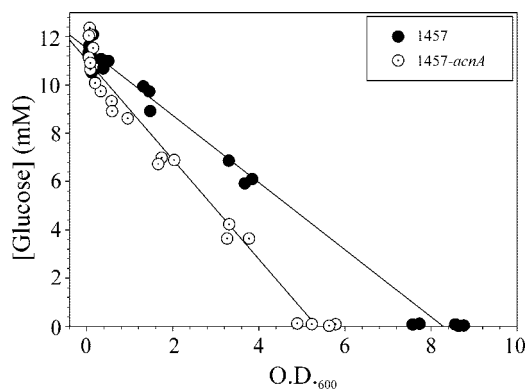
FIG. 2. TCA cycle inactivation redirects glucose carbons away from growth. The concentrations of glucose in the culture medium of *S. epidermidis* strains 1457 and 1457-*acnA* were plotted as a function of growth. The data are from three independent experiments, and the line is a linear regression of these data generated using SigmaPlot 10.0. O.D.$_{600}$, optical density at 600 nm.
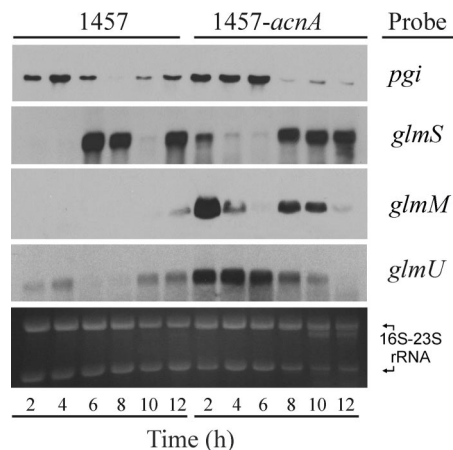

FIG. 3. Northern blot analysis of UDP-*N*-acetylglucosamine biosynthetic genes in *S. epidermidis* strains 1457 and 1457-*acnA*. At the indicated times during the growth cycle, total RNA was isolated from strains 1457 and 1457-*acnA*, and Northern blot analysis was performed using the indicated probes. To ensure that equivalent quantities of RNA were loaded, 23S and 16S rRNA were visualized by ethidium bromide staining and used as loading controls (bottom panel). The results are representative of at least two independent experiments.

(Table 3). In addition to increasing the carbon flow into branched-chain amino acid biosynthesis, the presence of a high concentration of glucono-1,5-lactone in strain 1457-*acnA* suggests that inactivation of the TCA cycle increased carbon flow into the pentose phosphate pathway.

NMR metabolomics indicated that TCA cycle inactivation redirected carbon into UDP-*N*-acetylglucosamine biosynthesis (Tables 3 and 4). If carbon were being redirected into UDP-*N*-acetylglucosamine biosynthesis, then it is likely that transcription of genes coding for the UDP-*N*-acetylglucosamine biosynthetic enzymes would be increased. To determine whether TCA cycle inactivation altered the transcription of UDP-*N*-acetylglucosamine biosynthetic genes, we probed total RNA for *pgi* (glucose-6-phosphate isomerase), *glmS* (glucosamine-6-phosphate synthase), *glmM* (phosphoglucosamine mutase), and *glmU* (UDP-*N*-acetylglucosamine pyrophosphorylase) (Fig. 3). Consistent with metabolomic data indicating an increased intracellular concentration of fructose-6-phosphate, transcription of *pgi* was slightly increased in *S. epidermidis* strain 1457-*acnA* relative to strain 1457 during the exponential growth phase. (Glucose-6-phosphate isomerase catalyzes the second step in glycolysis, specifically, the reversible isomerization of glucose-6-phosphate into fructose-6-phosphate.) Fructose-6-phosphate is the biosynthetic precursor of UDP-*N*-acetylglucosamine, whose biosynthesis is encoded within the genes *glmS*, *glmM*, and *glmU*. The exponential-growth-phase mRNA levels of *glmS*, *glmM*, and *glmU* were increased in strain 1457-*acnA* relative to strain 1457. Taken together, these data demonstrate that TCA cycle inactivation results in transcriptional changes that redirect carbon into *N*-acetylglucosamine biosynthesis.

In addition to providing biosynthetic intermediates, the TCA cycle generates ATP and reducing potential; therefore, a metabolic block in the TCA cycle will alter the energy status of the bacterium. As an indicator of the energy status, the intracellular concentrations of NAD$^+$, NADH, and ATP were determined for *S. epidermidis* strains 1457 and 1457-*acnA*. The intracellular concentration of ATP was lower in the aconitase mutant strain relative to the wild-type strain during both the exponential and postexponential growth phases (Fig. 4C). This decreased ATP concentration was likely due to decreased oxidative phosphorylation, as the intracellular concentrations of NAD$^+$ and NADH were significantly ($P < 0.01$) lower in the aconitase mutant strain than in the wild-type strain (Fig. 4A and B).

TCA cycle inactivation increases PIA accumulation. To determine whether TCA cycle inactivation resulted in increased synthesis of PIA, we assessed the relative amounts of cell-associated PIA in the *acnA* mutant, the complemented *acnA* mutant, and the wild-type strains using a PIA immunoblot assay (Fig. 5A and B). In addition, to facilitate comparison of the effect of TCA cycle inactivation on PIA accumulation with the inactivation of well-established regulators (i.e., IcaR, σ^B, and SarA), we determined the relative amounts of cell-associated PIA for isogenic strains that had *icaR*, *sarA*, or *sigB* genetically inactivated. In agreement with previous studies (9, 10, 26, 35, 74), we observed that mutations in the genes of positive regulators *sigB* and *sarA* decreased PIA accumulation relative to the wild-type strain, while inactivation of *icaR* increased PIA accumulation (Fig. 5A and B). Surprisingly, aconitase inactivation had a much greater effect on PIA synthesis than did inactivation of the well-studied repressor IcaR (Fig. 5A and B). Complementation of the *acnA* mutation restores PIA accumulation to that seen in the parental strain (Fig. 5A and B).

In *B. subtilis*, aconitase inactivation results in the accumulation of citric acid, which is partially responsible for blocking sporulation and causing a slight decrease in the growth rate (12). NMR metabolomics revealed an accumulation of citric acid in the aconitase mutant strain relative to the wild-type strain (see Fig. S1 and S2 in the supplemental material) (Tables 3 and 4), raising the possibility that the increased accumulation of PIA and the decreased growth rate of *S. epidermidis* strain 1457-*acnA* relative to strain 1457 might be due to citric acid-induced stress. To address these
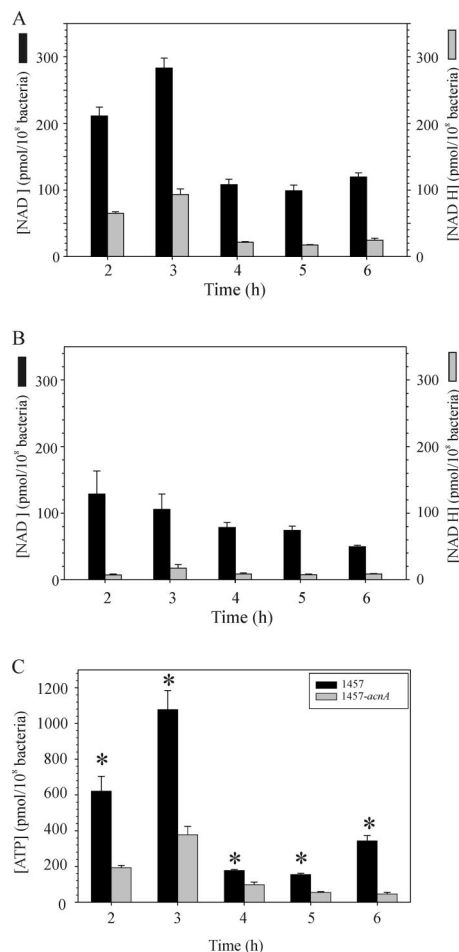
FIG. 4. Aconitase inactivation alters the redox and energy status of *S. epidermidis*. (A) At the indicated times during the growth cycle, intracellular concentrations of NAD and NADH were determined in *S. epidermidis* strain 1457. (B) Similarly, the concentrations of reduced and oxidized NAD were determined for strain 1457-*acnA*. (C) ATP concentrations were determined for strains 1457 and 1457-*acnA*. The results are presented as the means plus standard errors of the means (error bars) of duplicate determinations for at least two independent experiments.
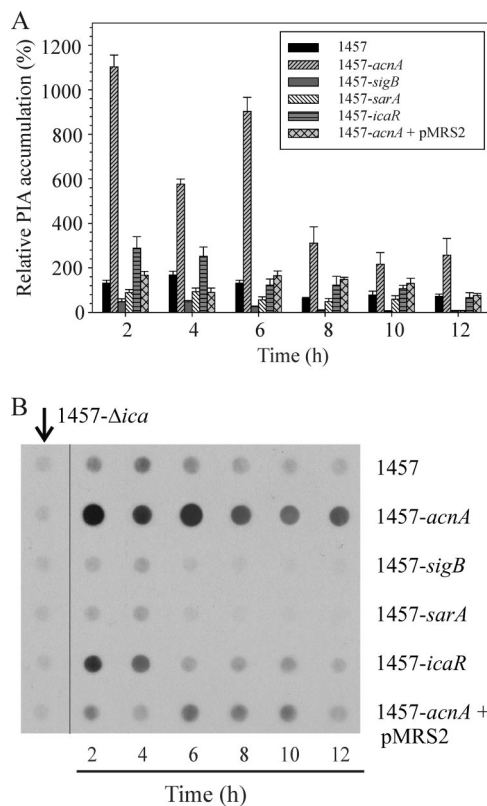

FIG. 5. TCA cycle inactivation increases PIA accumulation. (A) Relative amounts of cell-associated PIA were determined using a PIA immunoblot assay for *S. epidermidis* strains 1457, 1457-*acnA*, 1457-*sigB*, 1457-*sarA*, 1457-*icaR*, and 1457-*acnA* containing pMRS2 (1457-*acnA* + pMRS2). To determine the relative amounts of PIA, we defined the amount of PIA produced by strain 1457 at 2 h in one experiment as 100% and expressed all other amounts as relative to the amount at this 2-h point. The results are presented as the means plus standard errors of the means (error bars) for three independent experiments. (B) Representative immunoblot used for determining spot volumes. Strain 1457-Δ*ica*, which does not synthesize PIA, was used to determine the background density.

possibilities, we inactivated both citrate synthase (*citZ*) and isocitrate dehydrogenase (*citC*) in *S. epidermidis* strain 1457 and assessed growth and assayed for PIA accumulation (data not shown). Similar to the aconitase mutant strain, the *citCZ* double mutant dramatically increased PIA accumulation. Additionally, the *citCZ* double mutant had a decreased growth rate relative to the wild-type strain, but the growth rate was increased relative to strain 1457-*acnA* (data not shown), suggesting that citric acid accumulation was partially responsible for the slower growth of the aconitase mutant. Taken together, these data demonstrate that TCA cycle activity represses *S. epidermidis* PIA accumulation and that this effect is independent of citric acid.

TCA cycle activity represses *icaADBC* transcription. TCA cycle inactivation alters the metabolic status of *S. epidermidis* (Fig. 1A to D and 3 and Tables 3 and 4), raising the possibility that an *icaADBC* transcriptional regulator could

respond to the altered metabolic environment to increase *icaADBC* transcription. To determine whether the increased accumulation of PIA by the *acnA* mutant strain was due to altered *icaADBC* transcription, we examined *icaADBC* mRNA levels in *S. epidermidis* strains 1457 and 1457-*acnA*. In addition, *icaADBC* mRNA levels were determined for strain 1457 with mutations in *sigB*, *sarA*, or *icaR*. Consistent with the PIA immunoblot data (Fig. 5A and B), aconitase inactivation resulted in a very large increase in *icaADBC* transcription, or mRNA stability, relative to the isogenic wild-type strain (Fig. 6A and B), demonstrating that TCA cycle activity represses *icaADBC* transcription. In agreement with previous results, we observed that *sigB* and *sarA* inactivation repressed *icaADBC* transcription and that *icaR* inactivation derepressed *icaADBC* transcription (9, 11, 26). Interestingly, the extent of derepression in the 1457-*acnA* mutant strain was dramatically higher than seen in an isogenic *icaR* mutant (Fig. 6A and B), suggesting TCA cycle activity has a greater role in regulating *icaADBC* transcription than does IcaR. These data demonstrate that, like reg-
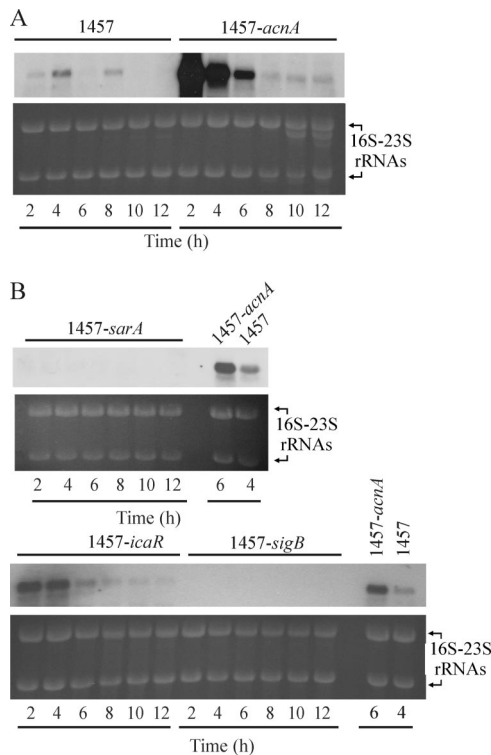
FIG. 6. TCA cycle inactivation derepresses *icaADBC* transcription. Total RNA was isolated from *S. epidermidis* strains 1457 and 1457-*acnA*, 1457-s*arA*, 1457-*icaR*, and 1457-*sigB*, and Northern blot analysis was performed using an *icaD*-specific probe. To make certain equivalent quantities of RNA were loaded, 23S and 16S rRNA were visualized by ethidium bromide staining and used as loading controls (bottom blots). To permit direct comparison of autoradiographs, total RNA from strains 1457-*acnA* and 1457 isolated at 6 h and 4 h postinoculation, respectively, were used to normalize the exposure times. (To minimize variation, the same preparations of RNA were used as exposure controls in all experiments.) The results are representative of at least two independent experiments.
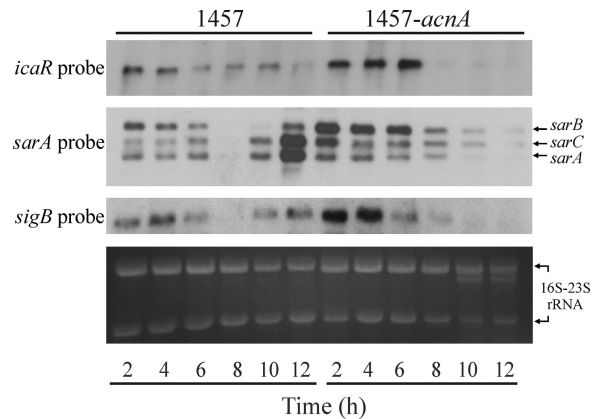

FIG. 7. Aconitase inactivation increases transcription of *icaR*, *sarA*, and *sigB*. Northern blot analysis with *icaR*, *sarA*, and *sigB* with DNA probes generated using primers shown in Table 2. To ensure that equivalent quantities of RNA were loaded, 23S and 16S rRNA were visualized by ethidium bromide staining and used as loading controls (bottom blot). The results are representative of at least two independent experiments.

ulation of the *lac* operon, *icaADBC* transcription is regulated by a catabolic process, specifically, the TCA cycle.

TCA cycle inactivation alters transcription of *icaR*, *sarA*, and *sigB*. As stated, transcription of *icaADBC* requires at least two positive effectors, SarA and σ^B, and one negative regulator, IcaR. The dramatic increase in *icaADBC* mRNA levels in the aconitase mutant strain relative to the wild-type strain could be due to an increased number of positive effectors or a decreased number of negative effectors. To determine whether aconitase inactivation altered transcription of the known regulators of *icaADBC* transcription, we probed total RNA isolated throughout the growth cycle for changes in the transcription of *sigB*, *sarA*, and *icaR* (Fig. 7). Surprisingly, aconitase inactivation increased transcription or mRNA stability of both positive regulators *sigB* and *sarA* and the negative regulator *icaR*. These data suggest that TCA cycle inactivation can alter the mRNA levels of the known regulators of PIA synthesis; however, they fail to establish that these regulators are involved in TCA cycle-mediated regulation of PIA synthesis. To determine whether IcaR, SarA, or σ^B is regulating PIA synthesis in response to TCA cycle-associated metabolic changes, *icaR*,

sarA, and *sigB* regulatory mutants of strain 1457 were incubated with 400 μM of the aconitase inhibitor fluorocitric acid, and PIA accumulation was assessed relative to the parental strain 1457 (Fig. 8.) The addition of fluorocitric acid to the culture medium of *S. epidermidis* strains 1457-*sigB* and 1457-*icaR* significantly ($P < 0.01$) increased the accumulation of PIA relative to the untreated control cultures. In strain 1457-*sarA*, the accumulation of PIA was similar irrespective of the presence of fluorocitric acid in the culture medium ($P > 0.05$). Overall, these data suggest that TCA cycle-mediated derepression of *ica* transcription and PIA synthesis occur independently of IcaR and σ^B. Furthermore, these data confirm that PIA synthesis requires SarA (10, 74) and at least one additional TCA cycle-responsive negative regulator.
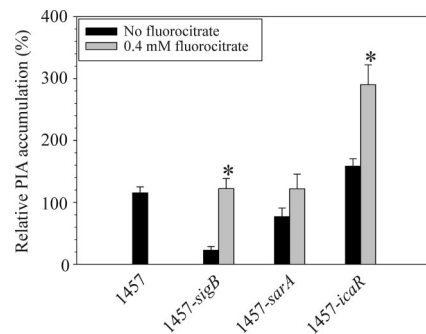

FIG. 8. Partial biochemical inhibition of aconitase increases PIA synthesis in *sigB* and *icaR* mutants. Bacterial cultures were incubated with 400 μM fluorocitric acid and grown for 2 h, and the relative amounts of cell-associated PIA were determined by a PIA immunoblot assay. The data are presented as the means plus standard errors of the means (error bars) from three independent experiments. Values that were significantly different ($P < 0.05$) from the value for the isogenic untreated control (0 μM fluorocitrate) are indicated by an asterisk.

DISCUSSION

Metabolic effect of TCA cycle activity on PIA biosynthesis. Glycolysis is the catabolic pathway that converts glucose into pyruvate, with the catabolic fate of pyruvate being determined by the availability of oxygen. Interestingly, the rate of glucose utilization by the wild-type *S. epidermidis* strain 1457 appears greater than the rate by strain 1457-*acnA* (Fig. 1C); however, these data fail to account for the number of bacteria in the medium. When this is taken into account, glucose utilization was greater in strain 1457-*acnA* than in strain 1457 (Fig. 2), suggesting that carbon flow through glycolysis might be greater in a TCA cycle mutant. If the amount of carbon flowing through glycolysis were greater in a TCA cycle mutant than in the parental strain, then the amount of acetate in the culture medium at the time when glucose was depleted should be greater in the mutant. Glucose was depleted in the wild-type and complemented strains after 5 h of growth; however, in strain 1457-*acnA*, glucose was depleted after 7 h of growth (Fig. 1C). Upon depletion of glucose, the concentrations of acetate in the culture medium were similar (14 to 16 mM) for all strains (Fig. 1D), suggesting that carbon flow through glycolysis was similar in the aconitase mutant and the wild-type strain. Additionally, because the concentrations of acetate were below 24 mM (if all glucose is processed through the glycolytic pathway, then a 2:1 stoichiometry of acetate to glucose should be maintained), the data confirm that carbon are flowing into other pathways. Consistent with these data, NMR metabolomics indicated that the exponential-growth-phase concentrations of acetic acid in strains 1457 and 1457-*acnA* were similar (Table 3). In addition to glycolysis, another major pathway staphylococci use for glucose catabolism is the pentose phosphate pathway (8, 70). The presence of glucono-1,5-lactone in the NMR metabolomic data (Table 3) suggests that carbon flow through the pentose phosphate pathway is increased in the TCA cycle mutant strain relative to the wild-type strain. One function of the pentose phosphate pathway is to provide the five-carbon intermediate for purine biosynthesis; hence, the increased carbon flow through the pentose phosphate pathway is likely linked to the decreased intracellular concentration of ATP in strain 1457-*acnA* relative to strain 1457 (Fig. 3). (De novo biosynthesis of ATP requires 5-phosphoribosyl-1-pyrophosphate. An important function of the pentose phosphate pathway is to provide biosynthetic intermediates for purine biosynthesis, namely, ribose-5-phosphate that is converted into 5-phosphoribosyl-1-pyrophosphate.)

NMR metabolomic data revealed an increased intracellular concentration of fructose-6-phosphate in the TCA cycle mutant relative to the wild-type strain (Table 3). Fructose-6-phosphate can undergo a transamination reaction to generate glucosamine-6-phosphate, a reaction catalyzed by glucosamine-6-phosphate synthase (*glmS*; EC 2.6.1.16). Phosphoglucosamine mutase (*glmM*; EC 5.4.2.10) catalyzes the reversible isomerization glucosamine-6-phosphate to glucosamine-1-phosphate. Glucosamine-1-phophaste is the substrate for the bifunctional enzyme UDP-*N*-acetylglucosamine pyrophosphorylase (*glmU*; EC 2.7.7.23 and EC 2.3.1.157) that catalyzes the acetylation and UTP-dependent activation of glucosamine-1-phosphate to generate UDP-*N*-acetylglucosamine. NMR metabolomics confirmed that *S. epidermidis* strain 1457-*acnA*

has a greater intracellular concentration of UDP-*N*-acetylglucosamine than strain 1457 does. In addition, transcription of *glmS*, *glmM*, and *glmU* is increased more during the exponential growth phase in the TCA cycle mutant than in the wild-type strain (Fig. 3). In total, these data demonstrate that TCA cycle inactivation increased the availability of the PIA monomer, UDP-activated *N*-acetylglucosamine and that this was partially due to transcriptional derepression of *N*-acetylglucosamine biosynthetic genes.

In addition to PIA synthesis, UDP-*N*-acetylglucosamine is critical for biosynthesis of the cell wall components teichoic acid and peptidoglycan. Inactivation of aconitase in *S. epidermidis* decreased the growth rate (Fig. 1B) and the number of bacteria produced per unit of glucose (Fig. 2), suggesting that UDP-*N*-acetylglucosamine was redirected from cell wall biosynthesis to PIA synthesis (Fig. 5A). Thus, the decreased growth rate of the aconitase mutant strain was likely due to a combination of increased competition for substrate (i.e., UDP-*N*-acetylglucosamine) by PIA biosynthetic enzymes and an accumulation of citric acid.

Regulatory effect of TCA cycle activity on PIA biosynthesis. Two common mechanisms by which bacteria control carbon flow are feedback inhibition of enzyme activity and regulation of enzyme synthesis. Undoubtedly, some of the metabolic changes arising from TCA cycle inactivation are the result of feedback inhibition of enzyme activity; however, by definition, the derepression of *icaADBC* transcription (Fig. 6A and B) must be at the regulatory level. Although the prospect that TCA cycle enzymes directly regulate *icaADBC* transcription is a possibility, it is more likely that regulation is being mediated by regulatory proteins responding to changes in the metabolic status of the bacteria. Metabolic regulation was one of the first bacterial regulatory modalities identified, resulting in thousands of studies addressing all aspects of regulation. This long history of research into metabolic regulation has identified a large number of regulatory proteins capable of responding to changes in the intracellular concentrations of molecules associated with TCA cycle activity, such as NADH (e.g., Rex [4], NmrA [39], and CcpA [21]), citric acid (CcpC [30, 33]), glutamate (GadX and GadW [75]), branched-chain amino acids (CodY [61]), and ATP (KinA [69]). These observations lead us to hypothesize that a regulatory protein or proteins respond to TCA cycle-associated metabolites and regulate *icaADBC* transcription and PIA synthesis.

TCA cycle inactivation increased the transcription or mRNA stability of the known regulators of *icaADBC* transcription, specifically, *sigB*, *sarA*, and *icaR* (Fig. 7). These data raise the possibility that TCA cycle-induced alterations in the metabolic status of the bacterium might be "sensed" by σ^B, SarA, or IcaR. Incubation of *S. epidermidis* strain 1457-*sigB* with a low concentration of the TCA cycle inhibitor fluorocitric acid restored PIA synthesis to wild-type levels (Fig. 8). This fluorocitrate-induced derepression of PIA synthesis in the *sigB* mutant strain is similar to that observed in an *S. epidermidis* *rsbU* mutant strain (RsbU is an activator of σ^B) treated with a PIA synthesis-stimulating concentration of ethanol (34). In that study, the authors found that ethanol could restore cell-associated PIA accumulation in an *rsbU* mutant strain to a level equivalent to that of the nonstimulated wild-type strain. Because ethanol is an inhibitor of TCA cycle activity (6, 37), we

hypothesize that the PIA synthesis-stimulating properties of ethanol may be due to its TCA cycle inhibitory properties.

Inactivation of *sarA* in *S. epidermidis* dramatically decreases *icaADBC* transcription (74) and PIA accumulation (26, 74) and results in a biofilm-negative phenotype (10). Because SarA is thought to be essential for PIA synthesis (74), the more likely outcome of incubating *S. epidermidis* strain 1457-*sarA* with fluorocitric acid would be equivalent PIA accumulation between the wild-type and *sarA* mutant strains. As expected, the amount of PIA produced by strain 1457-*sarA* was similar irrespective of the presence of fluorocitric acid (Fig. 8). These data are consistent with SarA being essential for PIA synthesis and/or being required for responding to TCA cycle-associated signals.

TCA cycle inactivation increased transcription or mRNA stability of *icaR* relative to the wild-type strain (Fig. 7). IcaR is a transcriptional repressor of *icaADBC* that was originally hypothesized to be involved in environmental regulation of PIA synthesis (9). For these reasons, IcaR appeared to be a possible candidate for responding to TCA cycle-induced metabolic changes. If IcaR were responding to TCA cycle-associated metabolic changes, then in an *icaR* mutant background, the synthesis of PIA should be unaffected by the presence of fluorocitric acid. Growth of strain 1457-*icaR* in the presence of a low concentration of fluorocitric acid significantly increased the accumulation of PIA (Fig. 8), demonstrating that a second repressor is involved in regulating PIA synthesis. It is likely that this second repressor is responding to TCA cycle-associated metabolic signals.

NMR metabolomics (Table 3) indicated that the intracellular concentrations of branched-chain amino acids were greater in the aconitase mutant strain than in the wild-type strain. In gram-positive bacteria, the intracellular concentrations of branched-chain amino acids control the expression of numerous genes, a mechanism requiring the CodY regulatory protein (25, 61, 66, 72). The affinity of CodY for its operator site is enhanced in response to high intracellular concentrations of GTP and branched-chain amino acids (54, 61). The more likely explanations for our data are that CodY is an activator of *icaADBC* transcription, CodY-mediated repression is not functioning in *S. epidermidis* during the exponential growth phase, or a positive effector, potentially SarA, can overcome CodY-mediated repression. We recently demonstrated that CodY is a repressor of PIA synthesis in the closely related species *S. aureus* (45); thus, it seems unlikely that CodY is an activator of *icaADBC* transcription in *S. epidermidis*. Investigations are under way to determine the function of CodY in regulating *S. epidermidis* PIA synthesis.

In gram-positive bacteria, carbon catabolite repression is primarily mediated by CcpA (28). Recently, CcpA was shown to activate transcription of *icaADBC* and increase the accumulation of PIA in *S. aureus* (60). In *B. subtilis*, CcpA regulatory activity is controlled by interactions with phosphorylated HPr or Crh and fructose-1,6,-bisphosphate or glucose-6-phosphate (67). NMR analysis indicated that TCA cycle inactivation increased the intracellular concentration of fructose-6-phosphate (Table 3). Fructose-6-phosphate is the biosynthetic precursor of UDP-*N*-acetylglucosamine. In addition to its importance in PIA biosynthesis, fructose-6-phosphate can be reversibly isomerized to glucose-6-phosphate by glucose-6-phosphate isomerase, resulting in CcpA activation. Taken together, these data lead us to hypothesize that TCA cycle inactivation increases CcpA-mediated activation of *icaADBC*.

Conclusion. TCA cycle activity is repressed during the exponential growth phase; however, a basal level of activity is present. As evidenced by the data in this study, disruption of this basal activity can have pronounced metabolic consequences. TCA cycle activity is regulated by the availability of nutrients, oxygen, and iron (8, 62, 65, 71, 76) and by certain stress-inducing stimuli, such as heat, ethanol, and antibiotics (6, 36, 73); thus, numerous external conditions can interfere with the basal TCA cycle activity and produce metabolic changes. The linkage of TCA cycle activity and exopolysaccharide synthesis and the susceptibility of the TCA cycle to environmental inactivation lead us to speculate that one mechanism by which staphylococci perceive external environmental change is through alterations in TCA cycle activity. Thus, we hypothesize that the TCA cycle acts as a novel signal transduction pathway to translate external stimuli/conditions into intracellular signals that can stimulate or repress the activity of regulatory proteins like CodY and CcpA.

REFERENCES

1. **Baughn, A. D., and M. H. Malamy.** 2002. A mitochondrial-like aconitase in the bacterium *Bacteroides fragilis*: implications for the evolution of the mitochondrial Krebs cycle. Proc. Natl. Acad. Sci. USA **99:**4662–4667.
2. **Begun, J., J. M. Gaiani, H. Rohde, D. Mack, S. B. Calderwood, F. M. Ausubel, and C. D. Sifri.** 2007. Staphylococcal biofilm exopolysaccharide protects against *Caenorhabditis elegans* immune defenses. PLoS Pathog. **3:**e57.
3. **Bischoff, M., P. Dunman, J. Kormanec, D. Macapagal, E. Murphy, W. Mounts, B. Berger-Bächi, and S. Projan.** 2004. Microarray-based analysis of the *Staphylococcus aureus* σ^B regulon. J. Bacteriol. **186:**4085–4099.
4. **Brekasis, D., and M. S. Paget.** 2003. A novel sensor of NADH/NAD$^+$ redox poise in *Streptomyces coelicolor* A3(2). EMBO J. **22:**4856–4865.
5. **Brückner, R.** 1997. Gene replacement in *Staphylococcus carnosus* and *Staphylococcus xylosus*. FEMS Microbiol. Lett. **151:**1–8.
6. **Chatterjee, I., G. A. Somerville, C. Heilmann, H. G. Sahl, H. H. Maurer, and M. Herrmann.** 2006. Very low ethanol concentrations affect the viability and growth recovery in post-stationary-phase *Staphylococcus aureus* populations. Appl. Environ. Microbiol. **72:**2627–2636.
7. **Cho, S. H., K. Naber, J. Hacker, and W. Ziebuhr.** 2002. Detection of the *icaADBC* gene cluster and biofilm formation in *Staphylococcus epidermidis* isolates from catheter-related urinary tract infections. Int. J. Antimicrob. Agents **19:**570–575.
8. **Collins, F. M., and J. Lascelles.** 1962. The effect of growth conditions on oxidative and dehydrogenase activity in *Staphylococcus aureus*. J. Gen. Microbiol. **29:**531–535.
9. **Conlon, K. M., H. Humphreys, and J. P. O'Gara.** 2002. *icaR* encodes a transcriptional repressor involved in environmental regulation of *ica* operon expression and biofilm formation in *Staphylococcus epidermidis*. J. Bacteriol. **184:**4400–4408.
10. **Conlon, K. M., H. Humphreys, and J. P. O'Gara.** 2004. Inactivations of *rsbU* and *sarA* by IS*256* represent novel mechanisms of biofilm phenotypic variation in *Staphylococcus epidermidis*. J. Bacteriol. **186:**6208–6219.
11. **Conlon, K. M., H. Humphreys, and J. P. O'Gara.** 2002. Regulation of *icaR* gene expression in *Staphylococcus epidermidis*. FEMS Microbiol. Lett. **216:**171–177.
12. **Craig, J. E., M. J. Ford, D. C. Blaydon, and A. L. Sonenshein.** 1997. A null mutation in the *Bacillus subtilis* aconitase gene causes a block in Spo0A-phosphate-dependent gene expression. J. Bacteriol. **179:**7351–7359.
13. **Cramton, S. E., M. Ulrich, F. Götz, and G. Döring.** 2001. Anaerobic conditions induce expression of polysaccharide intercellular adhesin in *Staphylococcus aureus* and *Staphylococcus epidermidis*. Infect. Immun. **69:**4079–4085.
14. **Cui, Q., I. A. Lewis, A. D. Hegeman, M. E. Anderson, J. Li, C. F. Schulte,

W. M. Westler, H. R. Eghbalnia, M. R. Sussman, and J. L. Markley. 2008. Metabolite identification via the Madison Metabolomics Consortium Database. Nat. Biotechnol. **26:**162–164.

15. **Dean, B. A., R. E. Williams, F. Hall, and J. Corse.** 1973. Phage typing of coagulase-negative staphylococci and micrococci. J. Hyg. (London) **71:**261–270.

16. **Deighton, M., and R. Borland.** 1993. Regulation of slime production in *Staphylococcus epidermidis* by iron limitation. Infect. Immun. **61:**4473–4479.

17. **Delaglio, F., S. Grzesiek, G. W. Vuister, G. Zhu, J. Pfeifer, and A. Bax.** 1995. NMRPipe: a multidimensional spectral processing system based on UNIX pipes. J. Biomol. NMR **6:**277–293.

18. **Dobinsky, S., K. Kiel, H. Rohde, K. Bartscht, J. K. Knobloch, M. A. Horstkotte, and D. Mack.** 2003. Glucose-related dissociation between *icaADBC* transcription and biofilm expression by *Staphylococcus epidermidis*: evidence for an additional factor required for polysaccharide intercellular adhesin synthesis. J. Bacteriol. **185:**2879–2886.

19. **Foster, T. J.** 1998. Molecular genetic analysis of staphylococcal virulence. Methods Microbiol. **27:**433–454.

20. **Garrett, D. S., R. Powers, A. M. Gronenborn, and G. M. Clore.** 1991. A common sense approach to peak picking in two-, three-, and four-dimensional spectra using automatic computer analysis of contour diagrams. J. Magn. Reson. **95:**214–220.

21. **Gaudu, P., G. Lamberet, S. Poncet, and A. Gruss.** 2003. CcpA regulation of aerobic and respiration growth in *Lactococcus lactis*. Mol. Microbiol. **50:**183–192.

22. **Götz, F.** 2002. Staphylococcus and biofilms. Mol. Microbiol. **43:**1367–1378.

23. **Gracia, E., A. Fernández, P. Conchello, J. L. Alabart, M. Pérez, and B. Amorena.** 1999. In vitro development of *Staphylococcus aureus* biofilms using slime-producing variants and ATP-bioluminescence for automated bacterial quantification. Luminescence **14:**23–31.

24. **Greene, C., D. McDevitt, P. Francois, P. E. Vaudaux, D. P. Lew, and T. J. Foster.** 1995. Adhesion properties of mutants of *Staphylococcus aureus* defective in fibronectin-binding proteins and studies on the expression of *fnb* genes. Mol. Microbiol. **17:**1143–1152.

25. **Guédon, E., P. Serror, S. D. Ehrlich, P. Renault, and C. Delorme.** 2001. Pleiotropic transcriptional repressor CodY senses the intracellular pool of branched-chain amino acids in *Lactococcus lactis*. Mol. Microbiol. **40:**1227–1239.

26. **Handke, L. D., S. R. Slater, K. M. Conlon, S. T. O'Donnell, M. E. Olson, K. A. Bryant, M. E. Rupp, J. P. O'Gara, and P. D. Fey.** 2007. SigmaB and SarA independently regulate polysaccharide intercellular adhesin production in *Staphylococcus epidermidis*. Can. J. Microbiol. **53:**82–91.

27. **Heilmann, C., O. Schweitzer, C. Gerke, N. Vanittanakom, D. Mack, and F. Götz.** 1996. Molecular basis of intercellular adhesion in the biofilm-forming *Staphylococcus epidermidis*. Mol. Microbiol. **20:**1083–1091.

28. **Henkin, T. M., F. J. Grundy, W. L. Nicholson, and G. H. Chambliss.** 1991. Catabolite repression of alpha-amylase gene expression in *Bacillus subtilis* involves a trans-acting gene product homologous to the *Escherichia coli lacI* and *galR* repressors. Mol. Microbiol. **5:**575–584.

29. **Jeng, W. Y., T. P. Ko, C. I. Liu, R. T. Guo, C. L. Liu, H. L. Shr, and A. H. Wang.** 2008. Crystal structure of IcaR, a repressor of the TetR family implicated in biofilm formation in *Staphylococcus epidermidis*. Nucleic Acids Res. **36:**1567–1577.

30. **Jourlin-Castelli, C., N. Mani, M. M. Nakano, and A. L. Sonenshein.** 2000. CcpC, a novel regulator of the LysR family required for glucose repression of the *citB* gene in *Bacillus subtilis*. J. Mol. Biol. **295:**865–878.

31. **Kanehisa, M., M. Araki, S. Goto, M. Hattori, M. Hirakawa, M. Itoh, T. Katayama, S. Kawashima, S. Okuda, T. Tokimatsu, and Y. Yamanishi.** 2008. KEGG for linking genomes to life and the environment. Nucleic Acids Res. **36:**D480–484.

32. **Karp, P. D., C. A. Ouzounis, C. Moore-Kochlacs, L. Goldovsky, P. Kaipa, D. Ahren, S. Tsoka, N. Darzentas, V. Kunin, and N. Lopez-Bigas.** 2005. Expansion of the BioCyc collection of pathway/genome databases to 160 genomes. Nucleic Acids Res. **33:**6083–6089.

33. **Kim, H. J., A. Roux, and A. L. Sonenshein.** 2002. Direct and indirect roles of CcpA in regulation of *Bacillus subtilis* Krebs cycle genes. Mol. Microbiol. **45:**179–190.

34. **Knobloch, J. K., K. Bartscht, A. Sabottke, H. Rohde, H. H. Feucht, and D. Mack.** 2001. Biofilm formation by *Staphylococcus epidermidis* depends on functional RsbU, an activator of the *sigB* operon: differential activation mechanisms due to ethanol and salt stress. J. Bacteriol. **183:**2624–2633.

35. **Knobloch, J. K., S. Jager, M. A. Horstkotte, H. Rohde, and D. Mack.** 2004. RsbU-dependent regulation of *Staphylococcus epidermidis* biofilm formation is mediated via the alternative sigma factor σ^B by repression of the negative regulator gene *icaR*. Infect. Immun. **72:**3838–3848.

36. **Kohanski, M. A., D. J. Dwyer, B. Hayete, C. A. Lawrence, and J. J. Collins.** 2007. A common mechanism of cellular death induced by bactericidal antibiotics. Cell **130:**797–810.

37. **Kornmann, H., P. Duboc, P. Niederberger, I. Marison, and U. von Stockar.** 2003. Influence of residual ethanol concentration on the growth of *Gluconacetobacter xylinus* I 2281. Appl. Microbiol. Biotechnol. **62:**168–173.

38. **Kozitskaya, S., S. H. Cho, K. Dietrich, R. Marre, K. Naber, and W. Ziebuhr.** 2004. The bacterial insertion sequence element IS*256* occurs preferentially in nosocomial *Staphylococcus epidermidis* isolates: association with biofilm formation and resistance to aminoglycosides. Infect. Immun. **72:**1210–1215.

39. **Lamb, H. K., K. Leslie, A. L. Dodds, M. Nutley, A. Cooper, C. Johnson, P. Thompson, D. K. Stammers, and A. R. Hawkins.** 2003. The negative transcriptional regulator NmrA discriminates between oxidized and reduced dinucleotides. J. Biol. Chem. **278:**32107–32114.

40. **Lauble, H., M. C. Kennedy, M. H. Emptage, H. Beinert, and C. D. Stout.** 1996. The reaction of fluorocitrate with aconitase and the crystal structure of the enzyme-inhibitor complex. Proc. Natl. Acad. Sci. USA **93:**13699–13703.

41. **Lowry, O. H., N. J. Rosebrough, L. Farr, and R. J. Randall.** 1951. Protein measurement with the Folin phenol reagent. J. Biol. Chem. **193:**267–275.

42. **Mack, D., W. Fischer, A. Krokotsch, K. Leopold, R. Hartmann, H. Egge, and R. Laufs.** 1996. The intercellular adhesin involved in biofilm accumulation of *Staphylococcus epidermidis* is a linear beta-1,6-linked glucosaminoglycan: purification and structural analysis. J. Bacteriol. **178:**175–183.

43. **Mack, D., N. Siemssen, and R. Laufs.** 1992. Parallel induction by glucose of adherence and a polysaccharide antigen specific for plastic-adherent *Staphylococcus epidermidis*: evidence for functional relation to intercellular adhesion. Infect. Immun. **60:**2048–2057.

44. **Maira-Litrán, T., A. Kropec, C. Abeygunawardana, J. Joyce, G. Mark III, D. A. Goldmann, and G. B. Pier.** 2002. Immunochemical properties of the staphylococcal poly-*N*-acetylglucosamine surface polysaccharide. Infect. Immun. **70:**4433–4440.

45. **Majerczyk, C. D., M. R. Sadykov, T. T. Luong, C. Lee, G. A. Somerville, and A. L. Sonenshein.** 2008. *Staphylococcus aureus* CodY negatively regulates virulence gene expression. J. Bacteriol. **190:**2257–2265.

46. **McCombie, H., and B. C. Saunders.** 1946. Fluoroacetates and allied compounds. Nature **158:**382–385.

47. **Mekalanos, J. J.** 1992. Environmental signals controlling expression of virulence determinants in bacteria. J. Bacteriol. **174:**1–7.

48. **National Nosocomial Infections Surveillance.** 2004. National Nosocomial Infections Surveillance (NNIS) System Report, data summary from January 1992 through June 2004, issued October 2004. Am. J. Infect. Control **32:**470–485.

49. **Novick, R. P.** 1991. Genetic systems in staphylococci. Methods Enzymol. **204:**587–636.

50. **Olson, M. E., K. L. Garvin, P. D. Fey, and M. E. Rupp.** 2006. Adherence of *Staphylococcus epidermidis* to biomaterials is augmented by PIA. Clin. Orthop. Relat. Res. **451:**21–24.

51. **Projan, S. J., and G. L. Archer.** 1989. Mobilization of the relaxable *Staphylococcus aureus* plasmid pC221 by the conjugative plasmid pGO1 involves three pC221 loci. J. Bacteriol. **171:**1841–1845.

52. **Rachid, S., K. Ohlsen, U. Wallner, J. Hacker, M. Hecker, and W. Ziebuhr.** 2000. Alternative transcription factor σ^B is involved in regulation of biofilm expression in a *Staphylococcus aureus* mucosal isolate. J. Bacteriol. **182:**6824–6826.

53. **Rachid, S., K. Ohlsen, W. Witte, J. Hacker, and W. Ziebuhr.** 2000. Effect of subinhibitory antibiotic concentrations on polysaccharide intercellular adhesin expression in biofilm-forming *Staphylococcus epidermidis*. Antimicrob. Agents Chemother. **44:**3357–3363.

54. **Ratnayake-Lecamwasam, M., P. Serror, K. W. Wong, and A. L. Sonenshein.** 2001. *Bacillus subtilis* CodY represses early-stationary-phase genes by sensing GTP levels. Genes Dev. **15:**1093–1103.

55. **Rupp, M. E.** 1997. Infections of intravascular catheters and vascular devices, p. 379–399. *In* K. B. Crossley and G. L. Archer (ed.), The staphylococci in human disease. Churchill-Livingstone, New York, NY.

56. **Rupp, M. E., J. S. Ulphani, P. D. Fey, K. Bartscht, and D. Mack.** 1999. Characterization of the importance of polysaccharide intercellular adhesin/hemagglutinin of *Staphylococcus epidermidis* in the pathogenesis of biomaterial-based infection in a mouse foreign body infection model. Infect. Immun. **67:**2627–2632.

57. **Rupp, M. E., J. S. Ulphani, P. D. Fey, and D. Mack.** 1999. Characterization of *Staphylococcus epidermidis* polysaccharide intercellular adhesin/hemagglutinin in the pathogenesis of intravascular catheter-associated infection in a rat model. Infect. Immun. **67:**2656–2659.

58. **Sambrook, J., E. F. Fritsch, and T. Maniatis.** 1989. Molecular cloning: a laboratory manual, 2nd ed. Cold Spring Harbor Laboratory Press, Cold Spring Harbor, NY.

59. **Schenk, S., and R. A. Laddaga.** 1992. Improved method for electroporation of *Staphylococcus aureus*. FEMS Microbiol. Lett. **73:**133–138.

60. **Seidl, K., C. Goerke, C. Wolz, D. Mack, B. Berger-Bächi, and M. Bischoff.** 2008. *Staphylococcus aureus* CcpA affects biofilm formation. Infect. Immun. **76:**2044–2050.

61. **Shivers, R. P., and A. L. Sonenshein.** 2004. Activation of the *Bacillus subtilis* global regulator CodY by direct interaction with branched-chain amino acids. Mol. Microbiol. **53:**599–611.

62. **Somerville, G., C. A. Mikoryak, and L. Reitzer.** 1999. Physiological characterization of *Pseudomonas aeruginosa* during exotoxin A synthesis: glutamate, iron limitation, and aconitase activity. J. Bacteriol. **181:**1072–1078.

63. **Somerville, G. A., S. B. Beres, J. R. Fitzgerald, F. R. DeLeo, R. L. Cole, J. S. Hoff, and J. M. Musser.** 2002. In vitro serial passage of *Staphylococcus*

aureus: changes in physiology, virulence factor production, and *agr* nucleotide sequence. J. Bacteriol. **184:**1430–1437.

64. **Somerville, G. A., M. S. Chaussee, C. I. Morgan, J. R. Fitzgerald, D. W. Dorward, L. J. Reitzer, and J. M. Musser.** 2002. *Staphylococcus aureus* aconitase inactivation unexpectedly inhibits post-exponential-phase growth and enhances stationary-phase survival. Infect. Immun. **70:**6373–6382.

65. **Somerville, G. A., B. Saïd-Salim, J. M. Wickman, S. J. Raffel, B. N. Kreiswirth, and J. M. Musser.** 2003. Correlation of acetate catabolism and growth yield in *Staphylococcus aureus*: implications for host-pathogen interactions. Infect. Immun. **71:**4724–4732.

66. **Sonenshein, A. L.** 2005. CodY, a global regulator of stationary phase and virulence in Gram-positive bacteria. Curr. Opin. Microbiol. **8:**203–207.

67. **Sonenshein, A. L.** 2007. Control of key metabolic intersections in *Bacillus subtilis*. Nat. Rev. Microbiol. **5:**917–927.

68. **Southern, E. M.** 1975. Detection of specific sequences among DNA fragments separated by gel electrophoresis. J. Mol. Biol. **98:**503–517.

69. **Stephenson, K., and J. A. Hoch.** 2001. PAS-A domain of phosphorelay sensor kinase A: a catalytic ATP-binding domain involved in the initiation of development in *Bacillus subtilis*. Proc. Natl. Acad. Sci. USA **98:**15251–15256.

70. **Strasters, K. C., and K. C. Winkler.** 1963. Carbohydrate metabolism of *Staphylococcus aureus*. J. Gen. Microbiol. **33:**213–229.

71. **Throup, J. P., F. Zappacosta, R. D. Lunsford, R. S. Annan, S. A. Carr, J. T. Lonsdale, A. P. Bryant, D. McDevitt, M. Rosenberg, and M. K. Burnham.** 2001. The *srhSR* gene pair from *Staphylococcus aureus*: genomic and proteomic approaches to the identification and characterization of gene function. Biochemistry **40:**10392–10401.

72. **Tojo, S., T. Satomura, K. Morisaki, J. Deutscher, K. Hirooka, and Y. Fujita.** 2005. Elaborate transcription regulation of the *Bacillus subtilis ilv-leu* operon involved in the biosynthesis of branched-chain amino acids through global regulators of CcpA, CodY and TnrA. Mol. Microbiol. **56:**1560–1573.

73. **Tomlins, R. I., M. D. Pierson, and Z. J. Ordal.** 1971. Effect of thermal injury on the TCA cycle enzymes of *Staphylococcus aureus* MF 31 and *Salmonella typhimurium* 7136. Can. J. Microbiol. **17:**759–765.

74. **Tormo, M. A., M. Martí, J. Valle, A. C. Manna, A. L. Cheung, I. Lasa, and J. R. Penadés.** 2005. SarA is an essential positive regulator of *Staphylococcus epidermidis* biofilm development. J. Bacteriol. **187:**2348–2356.

75. **Tramonti, A., M. De Canio, I. Delany, V. Scarlato, and D. De Biase.** 2006. Mechanisms of transcription activation exerted by GadX and GadW at the *gadA* and *gadBC* gene promoters of the glutamate-based acid resistance system in *Escherichia coli*. J. Bacteriol. **188:**8118–8127.

76. **Varghese, S., Y. Tang, and J. A. Imlay.** 2003. Contrasting sensitivities of *Escherichia coli* aconitases A and B to oxidation and iron depletion. J. Bacteriol. **185:**221–230.

77. **von Eiff, C., G. Peters, and C. Heilmann.** 2002. Pathogenesis of infections due to coagulase-negative staphylococci. Lancet Infect. Dis. **2:**677–685.

78. **Vuong, C., J. B. Kidder, E. R. Jacobson, M. Otto, R. A. Proctor, and G. A. Somerville.** 2005. *Staphylococcus epidermidis* polysaccharide intercellular adhesin production significantly increases during tricarboxylic acid cycle stress. J. Bacteriol. **187:**2967–2973.

79. **Vuong, C., S. Kocianova, J. M. Voyich, Y. Yao, E. R. Fischer, F. R. Deleo, and M. Otto.** 2004. A crucial role for exopolysaccharide modification in bacterial biofilm formation, immune evasion, and virulence. J. Biol. Chem. **24:**54881–54886.

80. **Vuong, C., J. M. Voyich, E. R. Fischer, K. R. Braughton, A. R. Whitney, F. R. DeLeo, and M. Otto.** 2004. Polysaccharide intercellular adhesin (PIA) protects *Staphylococcus epidermidis* against major components of the human innate immune system. Cell. Microbiol. **6:**269–275.

81. **Wu, S., H. de Lencastre, and A. Tomasz.** 1996. Sigma-B, a putative operon encoding alternate sigma factor of *Staphylococcus aureus* RNA polymerase: molecular cloning and DNA sequencing. J. Bacteriol. **178:**6036–6042.

82. **Xu, L., H. Li, C. Vuong, V. Vadyvaloo, J. Wang, Y. Yao, M. Otto, and Q. Gao.** 2006. Role of the *luxS* quorum-sensing system in biofilm formation and virulence of *Staphylococcus epidermidis*. Infect. Immun. **74:**488–496.

83. **Yanisch-Perron, C., J. Vieira, and J. Messing.** 1985. Improved M13 phage cloning vectors and host strains: nucleotide sequences of the M13mp18 and pUC19 vectors. Gene **33:**103–119.

84. **Ziebuhr, W., C. Heilmann, F. Götz, P. Meyer, K. Wilms, E. Straube, and J. Hacker.** 1997. Detection of the intercellular adhesion gene cluster (*ica*) and phase variation in *Staphylococcus epidermidis* blood culture strains and mucosal isolates. Infect. Immun. **65:**890–896.
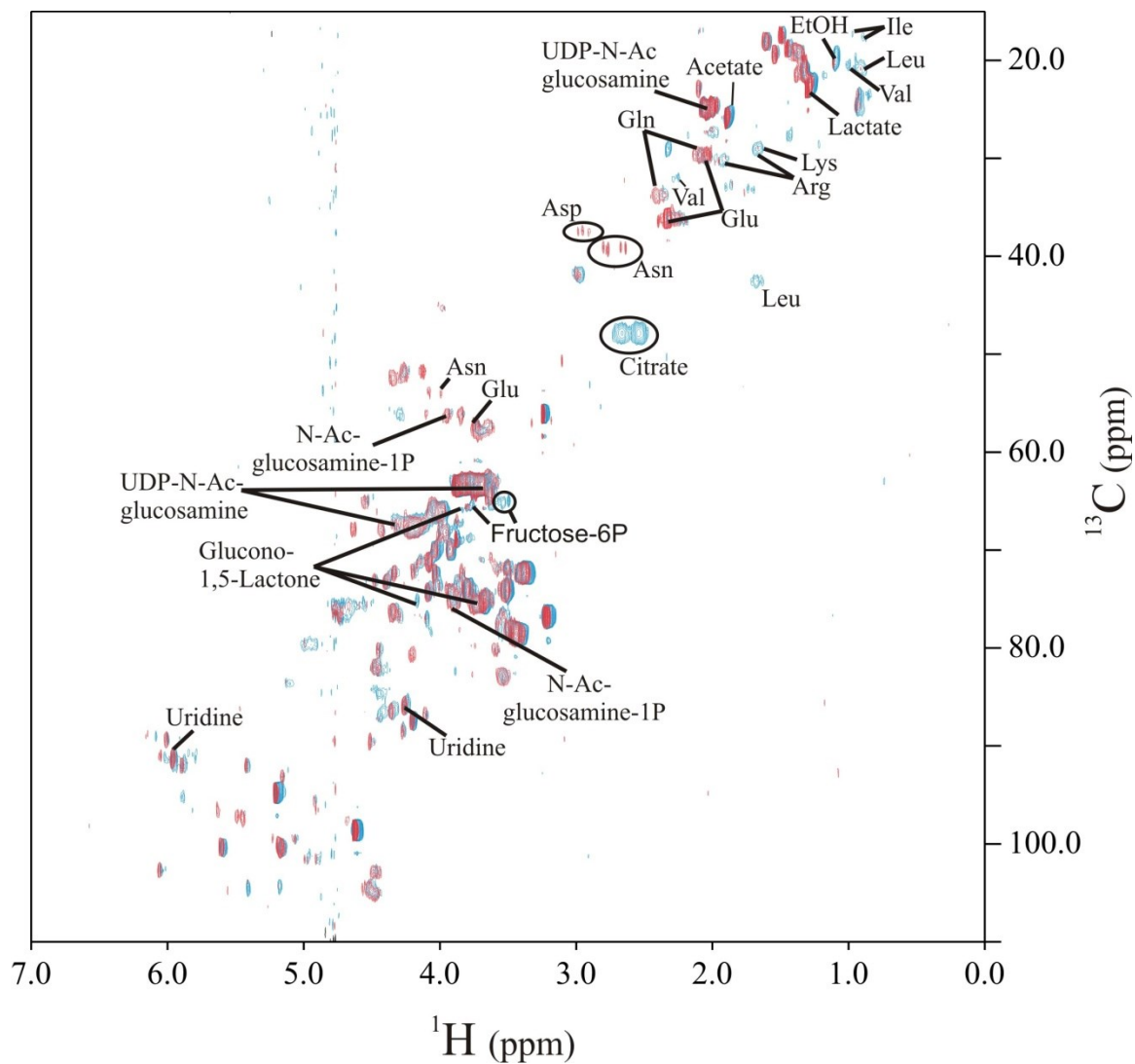
Supplemental Figure 1. NMR overlay spectra of *S. epidermidis* strain 1457 and strain 1457-*acnA* grown for 2 hours. The spectrum for strain 1457 is displayed in red and the spectrum for strain 1475-*acnA* is displayed in blue. Peaks of metabolites of interest are indicated within the figure. The data are representative of spectra collected from three independent cultures.
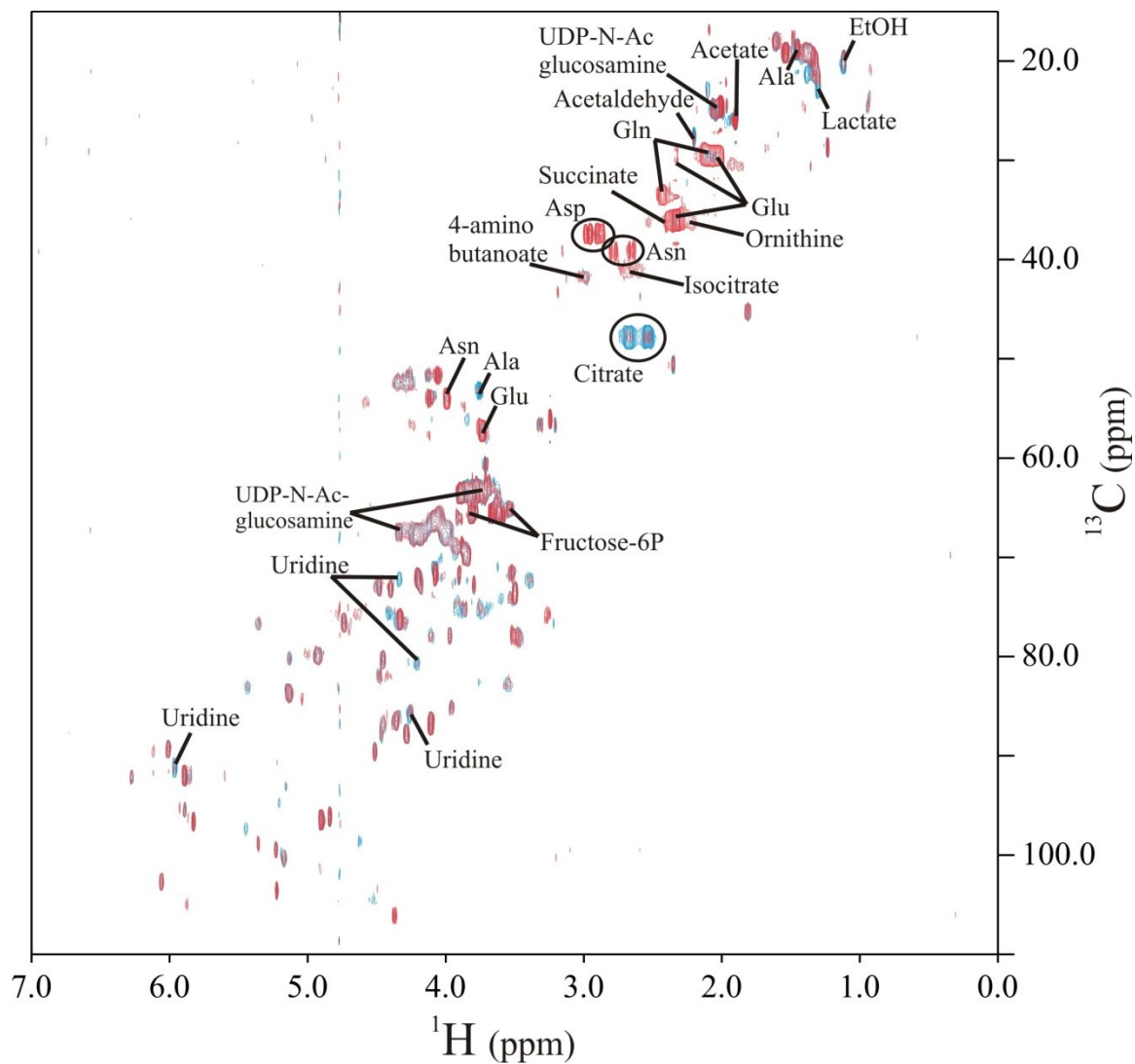
Supplemental Figure 2. NMR overlay spectra of *S. epidermidis* strain 1457 and strain 1457-*acnA* grown for 6 hours. The spectrum for strain 1457 is displayed in red and the spectrum for strain 1475-*acnA* is displayed in blue. Peaks of metabolites of interest are indicated within the figure. The data are representative of spectra collected from three independent cultures.